

Pressure and non-linear susceptibilities in QCD at finite chemical potentials

Rajiv V. Gavai* and Sourendu Gupta†

*Department of Theoretical Physics,
Tata Institute of Fundamental Research,
Homi Bhabha Road, Mumbai 400005, India.*

When the free energy density of QCD is expanded in a series in the chemical potential, μ , the Taylor coefficients are the non-linear quark number susceptibilities. We show that these depend on the prescription for putting chemical potential on the lattice, making all extrapolations in chemical potential prescription dependent at finite lattice spacing. To put bounds on the prescription dependence, we investigate the magnitude of the non-linear susceptibilities over a range of temperature, T , in QCD with two degenerate flavours of light dynamical quarks at lattice spacing $1/4T$. The prescription dependence is removed in quenched QCD through a continuum extrapolation, and the dependence of the pressure, P , on μ is obtained.

PACS numbers: 11.15.Ha, 12.38.Gc

TIFR/TH/03-07, hep-lat/0303013

One of the most important objects in the study of hot and dense hadronic matter is the phase diagram, particularly, the location of the critical end point, characterised by the temperature T_E and the chemical potential μ_E . Much effort has been expended recently on estimating these quantities at finite lattice spacing, a , using, implicitly [1] or explicitly [2, 3, 4], a Taylor series expansion of the free energy density, which needs the susceptibilities to an applied μ beyond linear order. Since present day heavy-ion collision experiments need $\mu \simeq 10\text{--}80$ MeV, i.e., baryon chemical potential $\mu_B \simeq 30\text{--}250$ MeV [5], it is also useful to ask whether linear susceptibilities, computed on the lattice at $\mu = 0$ are relevant to experiments at all.

In this paper we present the first investigation of these non-linear susceptibilities which allows us to quantify and remove lattice artifacts and present a continuum extrapolation. We explicitly construct a series expansion for P at $\mu > 0$, put limits on the region of linear response, i.e., of reliable extrapolations, and show that the $\mu = 0$ lattice computations are clearly relevant to experiments. An interesting sidelight is that there is strong evidence of short thermalisation times in the dense matter formed in these heavy-ion collisions [6], which may be related to large values of transport coefficients [7]. Most computations of such dynamical quantities are based on linear response theory. The success of the linear approximation in static quantities at fairly large driving also gives us confidence in using linear response theory for dynamics. We also argue that estimation of (T_E, μ_E) at finite a are necessarily prescription dependent.

The partition function of QCD at finite temperature T and chemical potentials μ_f for each flavour f can be written as

$$Z \equiv e^{-F/T} = \int \mathcal{D}U e^{-S(T)} \prod_f \text{Det } M(m_f, T, \mu_f). \quad (1)$$

F is the free energy, S is the gluon part of the action, M is the Dirac operator, each determinant is for one quark flavour and the temperature T enters through the

shape of the lattice and boundary conditions [8]. We shall work with a lattice discretisation and use staggered quarks [9]. In this work we shall only consider two degenerate flavours of quarks— $m_u = m_d = m$ [10], with chemical potentials μ_u and μ_d . The number densities, n_f , and the (linear) quark number susceptibilities, χ_{fg} , are the first and second derivatives of F/V with respect to μ_f and μ_g [11]. Since $P = F/V$ for a homogeneous system, the non-linear susceptibilities of order $n \geq 3$ are also the remaining Taylor coefficients of an expansion of P —

$$\chi_{fg\dots} = \frac{1}{V} \frac{\partial^n F}{\partial \mu_f \partial \mu_g \dots} = -\frac{T}{V} \frac{\partial^n \log Z}{\partial \mu_f \partial \mu_g \dots}, \quad (2)$$

where we construct the expansion around $\mu_f = 0$.

The derivatives of $\log Z$ can be related to $Z_{fg\dots}$, i.e., the derivatives of Z with respect to the chemical potentials μ_f , μ_g , etc., by the usual formulæ for taking connected parts. The only point to remember is that all the odd derivatives vanish by CP symmetry. Define operators \mathcal{O}_i by $Z_f = Z \langle \mathcal{O}_1 \rangle$ (the angular brackets denote averages over the ensemble defined by eq. 1) and $\mathcal{O}_{n+1} = \partial \mathcal{O}_n / \partial \mu_f$. Diagrammatic rules [12] for these operators, and the derivatives of Z , are—

1. Put down n vertices (each corresponding to a derivative of M with respect to μ_f) and label each with its flavour index.
2. Join the vertices by lines (each representing a quark) into sets of closed loops such that each loop contains only vertices of a single flavour. \mathcal{O}_i is denoted by a single loop joining i vertices.
3. For degenerate flavours and $\mu_f = 0$, the operators are labeled only by the topology, which is specified completely by the number of vertices per loop and the number of such loops. We denote each operator by the notation $\mathcal{O}_{ij\dots} = \mathcal{O}_i \mathcal{O}_j \dots$, where $i+j+\dots = n$.

4. For each n -th order derivative of Z , add all the operator topologies for fixed n with flavour-dependent multiplicity equal to the number of ways in which each topology arises given the flavour indices.

The new quantities that we now consider are the two third order derivatives $Z_{uuu} = Z\langle\mathcal{O}_3 + 3\mathcal{O}_{12} + \mathcal{O}_{111}\rangle$ and $Z_{uud} = Z\langle\mathcal{O}_{12} + \mathcal{O}_{111}\rangle$, the three fourth order derivatives $Z_{uuuu} = Z\langle\mathcal{O}_4 + 4\mathcal{O}_{13} + 3\mathcal{O}_{22} + 6\mathcal{O}_{112} + \mathcal{O}_{1111}\rangle$, $Z_{uuud} = Z\langle\mathcal{O}_{13} + 3\mathcal{O}_{112} + \mathcal{O}_{1111}\rangle$ and $Z_{uudd} = Z\langle\mathcal{O}_{22} + 2\mathcal{O}_{112} + \mathcal{O}_{1111}\rangle$, and the five corresponding susceptibilities. The operators contributing to these are shown in Figure 1. Beyond the second order, the number of distinct operator topologies is greater than the number of susceptibilities [12]; however by making N_f sufficiently large, all topologies up to any given order can be given a physical meaning.

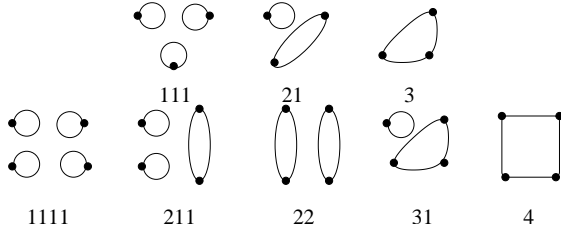


FIG. 1: All topologies which contribute to derivatives up to fourth order, and the notation for the corresponding operators.

A perturbative expansion in the continuum proceeds through an order-by-order enumeration of interaction terms. In the continuum the diagrams in Figure 1 are the leading order (ideal quark gas) part of the perturbative expansion of the susceptibilities, where each vertex corresponds to the insertion of a γ_0 (since the chemical potential enters the Lagrangian as $\gamma_0\mu_f$). Higher order Feynman diagrams correspond to dressing these loops by gluon attachments in all possible ways.

In the lattice theory the diagrams in Figure 1 stand for operator definitions which need further specification. They are not Feynman diagrams, but mnemonics for the process of taking derivatives of Z . Since, the coupling of Fermions to the chemical potential is non-linear [13], hence all derivatives of M exist and are non-zero in general. Using the identity $\text{Det } M = \exp(\text{Tr } \ln M)$ it is easy to get the usual expression $\mathcal{O}_1 = \text{Tr } M^{-1}M'$, where M' is the first derivative of M with respect to a chemical potential. Next, using the chain rule

$$\frac{dM^{-1}}{d\mu_f} = -M^{-1}M'M^{-1}, \quad (3)$$

which comes from the identity $MM^{-1} = 1$, we recover the relation $\mathcal{O}_2 = \text{Tr}(-M^{-1}M'M^{-1}M' + M^{-1}M'')$, where M'' is the second derivative of M with respect to the chemical potential. Higher operators can be derived by repeated application of the chain rule with eq. (3), and

involve higher derivatives of M , which we write as $M^{(n)}$. In particular, $\mathcal{O}_3 = \text{Tr}[2(M^{-1}M')^3 - 3M^{-1}M''M^{-1}M' + M^{-1}M^{(3)}]$ and $\mathcal{O}_4 = \text{Tr}[-6(M^{-1}M')^4 - 3(M^{-1}M'')^2 + 12M^{-1}M''(M^{-1}M')^2 - 4M^{-1}M^{(3)}M^{-1}M' + M^{-1}M^{(4)}]$. This completes the lattice definitions of the operators.

The prescription for putting chemical potential on the lattice is not unique. One can associate a factor $f(a\mu)$ for the propagation of a quark forward in time by one lattice spacing and a factor $g(a\mu)$ for the propagation of an antiquark. There are exactly four physical conditions that these two functions must satisfy [13]. In the absence of chemical potential the usual lattice theory must be recovered, hence $f(0) = g(0) = 1$. CP symmetry gives $f(-a\mu) = g(a\mu)$. Finiteness of the energy density is guaranteed if $f(a\mu)g(a\mu) = 1$. Finally, the correct continuum limit requires $f'(0) = 1$. These constraints imply the further relations, $f''(0) = 1$ and $f^{(n)}(0) = (-1)^n g^{(n)}(0)$, where the superscript n on f and g denotes the n -th derivative. All this guarantees that n_f and χ_{fg} are prescription independent.

The four conditions above also give relations between the remaining $f^{(n)}$, such as $f^{(4)} = 4f^{(3)} - 3$, but do not fix their numerical values. Since μ appears linearly in the continuum Lagrangian, these higher derivatives are all lattice artifacts. Any extra conditions imposed to fix them cannot be physical, and must remain at the level of prescription. The usual prescription, $f(a\mu) = \exp(a\mu)$ [14], which we call the HK prescription, gives $f^{(n)}(0) = 1$, but the alternative prescription $f(a\mu) = (1 + a\mu)/\sqrt{1 - a^2\mu^2}$ [15] gives $f^{(3)}(0) = 3$ and $f^{(4)}(0) = 9$.

This freedom has specific consequences for the third and higher derivatives of M , and through them for the non-linear susceptibilities, and hence for F , P and all quantities at finite μ and a . At $\mu_f = 0$, the odd derivatives of M are related by $M^{(n)} = f^{(n)}a^{n-2}M'$ and the even derivatives by $M^{(n)} = f^{(n)}a^{n-2}M''$. As a result, $\mathcal{O}_3 = \mathcal{O}_3^{HK} + \Delta f^{(3)}a^2\mathcal{O}_1$ and $\mathcal{O}_4 = \mathcal{O}_4^{HK} + 4\Delta f^{(3)}a^2\mathcal{O}_2$, where the superscript HK on an operator denotes its value obtained in the HK prescription and $\Delta f^{(3)} = f^{(3)} - 1$. Clearly, the prescription dependence, manifested as a non-vanishing $\Delta f^{(3)}$ at this order, disappears in the continuum limit, $a \rightarrow 0$. Since $\langle\mathcal{O}_1\rangle = 0$ at $\mu = 0$, the prescription dependence of $\langle\mathcal{O}_3\rangle$ is invisible. We find that $\chi_{uuud} = \chi_{uuud}^{HK} + \Delta f^{(3)}(\chi_{ud}/T^2)/N_t^2$. Since χ_{ud} vanishes within errors, as we show later, χ_{uuud} turns out to be effectively prescription independent. From the relation for \mathcal{O}_4 we find, on varying N_t at fixed T ,

$$\chi_{uuuu} = \chi_{uuuu}^{HK} + \Delta f^{(3)}\left(\frac{\chi_{uu}}{T^2}\right)\left(\frac{4}{N_t^2}\right). \quad (4)$$

Finally, χ_{uudd} involves neither $M^{(3)}$ nor $M^{(4)}$, and hence is prescription independent. The prescription dependence of other susceptibilities can be systematically worked out, and it can be shown exactly as above that they become physical only in the continuum. Mixed derivatives of T and μ also have similar behaviour.

T/T_c	m_V/T	$10^6 \chi_{ud}/T^2$	$10^6 \chi_{uuud}$	$10^4 \chi_{uudd}$	μ_*^{HK}/T
1.0	0.2	6 (30)	4 (17)	7 (1)	3.20 (3)
	0.1	8 (42)	7 (33)	9 (2)	3.31 (5)
	0.03	11 (84)	20 (172)	11 (2)	3.38 (4)
1.5	0.2	-0.3 (423)	-0.7 (116)	0.107 (3)	3.73 (1)
	0.1	0.6 (431)	-0.6 (128)	0.105 (3)	3.84 (1)
	0.03	-0.07 (433)	-0.5 (166)	0.106 (3)	3.86 (2)
2.0	0.2	2 (36)	0.5 (85)	0.097 (3)	3.83 (1)
	0.1	2 (36)	0.5 (89)	0.098 (3)	3.87 (1)
	0.03	1 (35)	0.6 (82)	0.096 (3)	3.78 (2)
3.0	0.2	0.6 (19)	0.1 (5)	0.032 (2)	3.87 (1)
	0.1	0.6 (20)	0.1 (5)	0.033 (2)	3.88 (2)
	0.03	0.6 (20)	0.1 (5)	0.033 (2)	3.88 (2)

TABLE I: Results in two flavour QCD with sea quark $m/T_c = 0.1$. For $T = T_c$ the results are based on 2017 configurations, for $1.5T_c$ on 370, for $2T_c$ on 126 and for $3T_c$ on 60. At T_c and $3T_c$ 100 noise vectors were used.

If the dependence on a of each susceptibility were known in any scheme, then one could write down an improved prescription by removing finite a effects systematically. In other schemes every quantity is potentially prescription dependent at finite lattice spacing. However, along the line $\mu_u = \mu_d = \mu$, the Taylor series expansion of P can be written in the form

$$\frac{\Delta P}{T^4} = \left(\frac{\chi_{uu}}{T^2}\right) \left(\frac{\mu}{T}\right)^2 \left[1 + \left(\frac{\mu/T}{\mu_*/T}\right)^2 + \mathcal{O}\left(\frac{\mu^4}{\mu_*^4}\right)\right], \quad (5)$$

where $\Delta P = P(\mu) - P(\mu = 0)$, and

$$\frac{\mu_*}{T} = \sqrt{\frac{12\chi_{uu}/T^2}{|\chi_{uuuu}|}}, \quad (6)$$

since χ_{uudd} turns out to be smaller even than the errors in χ_{uuuu} . If the series in eq. (5) is well behaved, i.e.. sixth and higher order susceptibilities are not much larger than χ_{uuuu} , then this expansion must be well approximated by the leading term for $\mu \ll \mu_*$ in every prescription, and hence be effectively independent of prescription [16]. However, the series expansion must fail to converge in the vicinity of a phase transition; therefore estimates of (T_E, μ_E) on finite lattices must be prescription dependent. Computation of the continuum limit of several terms in the double series for $F(T, \mu)$ may allow us to use series extrapolation methods to identify (T_E, μ_E) in the continuum limit.

We turn now to our numerical simulations. For dynamical sea quark mass $m/T_c = 0.1$ we studied the higher order susceptibilities at $T = T_c$ on a 4×10^3 lattice, $1.5T_c$ and $2T_c$ on 4×12^3 lattices, and $3T_c$ on a 4×14^3 lattice [17]. All the simulations were performed using the hybrid R-algorithm [18] with molecular dynamics trajectories integrated over one unit of MD time using a leap-frog

T/T_c	N_t	$10^6 \chi_{ud}/T^2$	$10^6 \chi_{uuud}$	μ_*^{HK}/T
1.5	4	2 (28)	-0.7 (56)	3.81 (2)
	8	0.2 (15)	0.2 (13)	4.36 (4)
	10	-0.4 (77)	0.04 (64)	4.47 (4)
	12	-0.5 (5)	0.00 (30)	4.55 (4)
	14	0.9 (58)	0.00 (24)	4.56 (4)
	∞	—	—	4.67 (4)
2.0	6	0.2 (67)	0.2 (10)	4.11 (1)
	8	-0.3 (115)	0.1 (13)	4.32 (5)
	10	-0.3 (76)	0.007 (49)	4.45 (3)
	12	0.0 (57)	0.00 (34)	4.56 (3)
	14	-0.2 (43)	0.00 (17)	4.59 (4)
	∞	—	—	4.76 (4)
3.0	4	2 (25)	0.8 (44)	3.85 (1)
	8	2 (4)	0.1 (4)	4.25 (5)
	10	-0.6 (14)	-0.04 (11)	4.40 (3)
	12	-0.1 (17)	-0.02 (7)	4.48 (4)
	14	-0.2 (8)	0.00 (3)	4.51 (2)
	∞	—	—	4.62 (1)

TABLE II: Results in quenched QCD with $m_v/T_c = 0.1$. Quadratic extrapolations to the continuum limit, $N_t = \infty$, from the last three points, are shown.

algorithm with time step of 0.01 units. At T_c autocorrelations of the Wilson line and the quark condensate were found to be between 150 and 250 trajectories. With over 2000 saved configurations separated by 10 trajectories each, this gave the equivalent of about 100 independent configurations. For $T > T_c$ the autocorrelations were all less than 10 trajectories, and hence all the saved configurations can be considered statistically independent.

Quark number susceptibilities were evaluated in the HK prescription on stored configurations using valence quark masses $m_V/T_c = 0.2, 0.1$ and 0.03 . The smallest valence quark mass is chosen such that the ratio of the $(T = 0)$ rho and pion masses reaches its physical value 0.2 at the lattice spacing $a = 1/4T_c$. All quark-line disconnected diagrams of the kind needed for these measurements are evaluated using a straightforward extension of the stochastic method given for χ_{ud} in [19] using 10 to 100 noise vectors per configuration [20]. Our results for the non-linear susceptibilities which do not vanish by symmetry are shown in Table I. It is clear that of these only χ_{uudd} and χ_{uuuu} , are non-zero with statistical significance. Comparing them to computations with sea quark mass $m/T_c = 0.2$ and various volumes, we concluded that they are free of sea quark mass and finite volume effects. Also note the stability in physical quantities as m_v/T_c decreases from 0.1 to 0.03.

With present day computer resources the continuum limit is hard to take in QCD with dynamical quarks. To investigate this limit we have evaluated the same quanti-

ties in quenched QCD for $T \geq 1.5T_c$ where the difference in the order of transitions is immaterial [21]. The run parameters are exactly as in [19]. Our results are shown in Table II. Comparison with the dynamical quark simulations at $a = 1/4T$ shows that quenching artifacts are small in the quantities we study. The range of applicability of the linear approximation, μ_*^{HK}/T , also increases with N_t , showing that in the HK prescription finite a effects in χ_{uuuu} (which is positive in both dynamical and quenched QCD) are larger than in χ_{uu} . χ_{uudd} remains significantly non-zero on all the lattices, and there is some evidence that it becomes negative in the continuum [22]. We shall present more detailed studies in the future. Finally, the results for $N_t = 4$ are very similar in the quenched and dynamical theories, leading us to believe that the continuum limits will also be close.

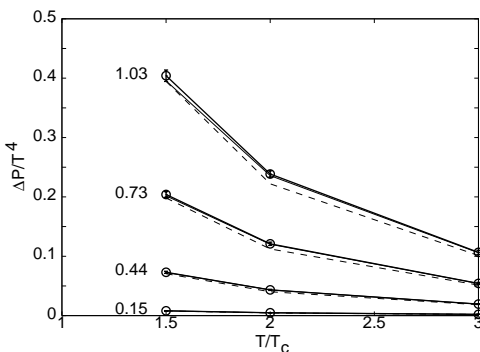


FIG. 2: $\Delta P/T^4$ as a function of T/T_c for the values of μ/T_c shown. Continuum results correct to $\mathcal{O}(\mu^4)$ (full lines) and $\mathcal{O}(\mu^2)$ (dotted lines) are shown. $N_t = 4$ results, in the HK prescription, correct to $\mathcal{O}(\mu^4)$ and multiplied by 0.47 to compensate for finite a effects in χ_{uu} are shown with dashed lines.

$\Delta P/T^4$ obtained in quenched QCD, using values of χ_{uu} from [19] and μ_*/T obtained here, are shown in Figure 2. In terms of dimensionless variables, the results in quenched and dynamical QCD are not expected to differ by more than 5–10% [23], implying that at RHIC, where $\mu/T_c = 0.06$, the effect of finite μ is negligible. For $\mu/T_c \simeq 0.45$, relevant to SPS energies, the effects of $\mu > 0$ are more significant, but can still be reliably extracted using only the leading term of eq. (5). For $\mu \geq 2T_c$, higher order terms become significant, and the $N_t = 4$ results, even after correcting for finite a effects in χ_{uu} , are quite different from the continuum values.

In conclusion, we have studied non-linear susceptibilities and shown that they are prescription dependent at finite lattice spacing. For $a = 1/4T$ the numerical results for QCD with and without dynamical quarks are similar, and we find the continuum limit of some of these quan-

ties in the quenched theory. It would be interesting to compare them with perturbation theory. We use these quantities to compute the corrections to the pressure at finite μ in the continuum limit. Our results permit reliable extrapolation up to $\mu \simeq T_c$. We have argued that the critical end point (T_E, μ_E) in the continuum limit may be accessible after computation of a larger number of these non-linear susceptibilities.

We would like to thank J.-P. Blaizot for discussions.

* Electronic address: gavai@tifr.res.in

† Electronic address: sgupta@tifr.res.in

- [1] Z. Fodor and S. D. Katz, *J. H. E. P.*, 03 (2002) 014.
- [2] C. R. Allton *et al.*, *Phys. Rev.*, D 66 (2002) 074507.
- [3] M. D'Elia and M.-P. Lombardo, hep-lat/0209146.
- [4] P. De Forcrand and O. Philipsen, *Nucl. Phys.*, B642 (2002) 290.
- [5] J. Cleymans, *J. Phys.*, G 28 (2002) 1575.
- [6] See, for example, U. Heinz, nucl-th/0212004.
- [7] S. Gupta, hep-lat/0301006.
- [8] Z is, of course, real and positive even for $\mu > 0$. In the quenched theory valence quarks exist and μ acts on them.
- [9] The determinant for each flavour is obtained as usual by taking the fourth root of each staggered quark determinant. As a result, there is a factor 1/4 for each quark loop evaluated with staggered quarks.
- [10] At vanishing μ , the effects of breaking the vector part of the flavour symmetry are small; see R. V. Gavai and S. Gupta, *Phys. Rev.*, D 66 (2002) 094510.
- [11] S. Gottlieb *et al.*, *Phys. Rev. Lett.* 59 (1987) 2247.
- [12] S. Gupta, *Acta Phys. Pol.*, B 33 (2002) 4259.
- [13] R. V. Gavai, *Phys. Rev. D* 32 (1985) 519.
- [14] P. Hasenfratz and F. Karsch, *Phys. Lett.*, B 125 (1983) 308.
- [15] N. Bilic and R. V. Gavai, *Z. Phys.*, C 23 (1984) 77.
- [16] Interestingly, at finite isospin density ($\mu_u = -\mu_d = \mu_3/2$) the expression for $\Delta P/T^4$ is also given by eq. (5). For imaginary μ_B , $\Delta P/T^4$ is negative and the higher order terms in eq. (5) alternate in sign.
- [17] T_c stands for the crossover temperature in 2 flavour QCD with finite mass quarks, and the critical temperature in quenched QCD.
- [18] S. Gottlieb *et al.*, *Phys. Rev.*, D 35 (1987) 2531.
- [19] R. V. Gavai and S. Gupta, *Phys. Rev. D* 67 (2003) 034501.
- [20] Our results are stable under change of such algorithmic parameters.
- [21] R. V. Gavai, S. Gupta and P. Majumdar, *Phys. Rev. D* 65 (2002) 054506.
- [22] A perturbative computation shows χ_{uudd} to be negative and much smaller in magnitude than χ_{uu}/T^2 (J.-P. Blaizot, private communication).
- [23] See also, Z. Fodor *et al.*, hep-lat/0208078.